

Diphoton Decay Excess and 125 GeV Higgs Boson in Gauge-  
Higgs Unification

N. Maru – Keio University, Hiyoshi

N. Okada – University of Alabama

Deposited 05/16/2019

Citation of published version:

Maru, N., Okada, N. (2013): Diphoton Decay Excess and 125 GeV Higgs Boson in Gauge-  
Higgs Unification. *Physical Review D*, 87(9).

DOI: <https://doi.org/10.1103/PhysRevD.87.095019>

**Diphoton decay excess and 125 GeV Higgs boson in gauge-Higgs unification**Nobuhito Maru<sup>1</sup> and Nobuchika Okada<sup>2</sup><sup>1</sup>*Department of Physics, and Research and Education Center for Natural Sciences,  
Keio University, Hiyoshi, Yokohama 223-8521, Japan*<sup>2</sup>*Department of Physics and Astronomy, University of Alabama, Tuscaloosa, Alabama 35487, USA  
(Received 27 March 2013; published 31 May 2013)*

In the context of the gauge-Higgs unification scenario in a 5-dimensional flat spacetime, we investigate Higgs boson production via gluon fusion and its diphoton decay mode at the LHC. We show that the signal strength of the Higgs diphoton decay mode observed at ATLAS and CMS, which is considerably larger than the Standard Model expectation, can be explained by a simple gauge-Higgs unification model with color-singlet bulk fermions to which a half-periodic boundary condition is assigned. The bulk fermions also play a crucial role in reproducing the observed Higgs boson mass around 125 GeV.

DOI: [10.1103/PhysRevD.87.095019](https://doi.org/10.1103/PhysRevD.87.095019)

PACS numbers: 11.10.Kk, 11.30.Qc, 12.60.Fr, 14.80.Bn

**I. INTRODUCTION**

It was recently announced by ATLAS [1] and CMS [2] collaborations that a Higgs(-like) boson was discovered at the Large Hadron Collider (LHC). Although the observed data for a variety of Higgs boson decay modes are found to be consistent with the Standard Model (SM) expectations, the diphoton decay mode shows the signal strength considerably larger than the SM prediction. Since the Higgs-to-diphoton coupling arises at the quantum level even in the SM, there is a good chance that the deviation originates from a certain new physics effect. This has motivated many recent studies for explanation of the deviation in various extensions of the SM with supersymmetry [3] or without supersymmetry [4].

In this paper, we investigate Higgs production via the gluon fusion and its diphoton decay in gauge-Higgs unification (GHU) [5]. The GHU scenario offers a solution to the gauge hierarchy problem without invoking supersymmetry, where the SM Higgs doublet is identified as an extra spatial component of the gauge field in higher dimensional theory. The scenario predicts various finite physical observables such as Higgs potential [6,7],  $H \rightarrow gg, \gamma\gamma$  [8,9], the anomalous magnetic moment  $g - 2$  [10], and the electric dipole moment [11], thanks to the higher dimensional gauge symmetry, irrespective of the nonrenormalizable theory.

In our previous paper [8] based on a simple GHU model, we have calculated loop contributions of Kaluza-Klein (KK) modes to the Higgs-to-digluon and Higgs-to-diphoton couplings and found that the KK mode contributions are destructive to the SM contributions by corresponding SM particles. This is a remarkable feature of the GHU, closely related to the absence of the quadratic divergence in Higgs self-energy corrections. In this paper we revisit this analysis for a simple extension of our previous GHU model. Introducing color-singlet bulk fermions with a half-periodic boundary condition, we investigate their effects on the Higgs-to-diphoton coupling and Higgs boson mass. We will show that the bulk fermions

of certain representations of the bulk gauge group can easily enhance the Higgs-to-diphoton coupling with appropriately chosen electric charges. The bulk fermions also play a crucial role to achieve a Higgs boson mass around 125 GeV. Without the bulk fermions, the Higgs boson mass is predicted to be too small, less than 100 GeV.

The plan of this paper is as follows. In the next section, we consider a 5-dimensional GHU model based on the gauge group  $SU(3) \times U(1)'$  with an orbifold  $S^1/Z_2$  compactification [12,13]. As simple explicit examples, we introduce color-singlet bulk fermions of **10** and **15** representations and impose a half-periodic boundary condition for them.  $U(1)'$  charges for the bulk fermions are appropriately assigned. In this context, we calculate Higgs production via gluon fusion and diphoton decay processes. The KK modes of the bulk fermions contribute to the Higgs-to-diphoton coupling constructively to the  $W$ -boson loop corrections in the SM and enhance the Higgs diphoton branching ratio. The magnitude of enhancement is determined by  $U(1)'$  charges and the representation of the bulk fermion, and a suitable choice of them can account for the observed signal strength of Higgs diphoton decay mode. In Sec. III, we estimate the Higgs boson mass using a 4-dimensional effective theory approach developed in Ref. [14], where the Higgs boson mass is determined via a 1-loop renormalization group equation (RGE) of the Higgs quartic coupling with the ‘‘gauge-Higgs condition’’ [14]. We find that the introduced bulk fermions play a crucial role to achieve a Higgs boson mass around 125 GeV through the RGE running of the Higgs quartic coupling. Section IV is devoted to the conclusions.

**II. HIGGS PRODUCTION AND  
DIPHOTON DECAY IN GHU**

We consider a GHU model based on the gauge group  $SU(3) \times U(1)'$  in a 5-dimensional flat space-time with orbifolding on  $S^1/Z_2$  with radius  $R$  of  $S^1$ . In our setup of bulk fermions, we follow Ref. [13]: the up-type quarks

except for the top quark, the down-type quarks and the leptons are embedded, respectively, into **3**,  $\bar{\mathbf{6}}$ , and **10** representations of  $SU(3)$ . In order to realize the large top Yukawa coupling, the top quark is embedded into a rank 4 representation of  $SU(3)$ , namely  $\bar{\mathbf{15}}$ . The extra  $U(1)'$  symmetry works to yield the correct Weinberg angle, and the SM  $U(1)_Y$  gauge boson is given by a linear combination between the gauge bosons of the  $U(1)'$  and the  $U(1)$  subgroup in  $SU(3)$  [12].<sup>1</sup> We assign appropriate  $U(1)'$  charges for bulk fermions to give the correct hypercharges for the SM fermions.

The boundary conditions should be suitably assigned to reproduce the SM fields as the zero modes. While a periodic boundary condition corresponding to  $S^1$  is taken for all of the bulk SM fields, the  $Z_2$  parity is assigned for gauge fields and fermions in the representation  $\mathcal{R}$  by using the parity matrix  $P = \text{diag}(-, -, +)$  as

$$A_\mu(-y) = P^\dagger A_\mu(y) P, \quad A_y(-y) = -P^\dagger A_y(y) P, \\ \psi(-y) = \mathcal{R}(P)\psi(y) \quad (1)$$

where the subscript  $\mu$  ( $y$ ) denotes the 4-dimensional (5-dimensional) component. With this choice of parities, the  $SU(3)$  gauge symmetry is explicitly broken to  $SU(2) \times U(1)$ . A hypercharge is a linear combination of  $U(1)$  and  $U(1)'$  in this setup. One may think that the  $U(1)_X$  gauge boson which is orthogonal to the hypercharge  $U(1)_Y$  also has a zero mode. However, the  $U(1)_X$  symmetry is anomalous in general and broken at the cutoff scale and hence, the  $U(1)_X$  gauge boson has a mass of order of the cutoff scale [12]. As a result, zero-mode vector bosons in the model are only the SM gauge fields.

Off-diagonal blocks in  $A_y$  have zero modes because of the overall sign in Eq. (1), which corresponds to an  $SU(2)$  doublet. In fact, the SM Higgs doublet ( $H$ ) is identified as

$$A_y^{(0)} = \frac{1}{\sqrt{2}} \begin{pmatrix} 0 & H \\ H^\dagger & 0 \end{pmatrix}. \quad (2)$$

The KK modes of  $A_y$  are eaten by KK modes of the SM gauge bosons and enjoy their longitudinal degrees of freedom like the usual Higgs mechanism.

The parity assignment provides the SM fermions as massless modes, but it also leaves exotic fermions massless. Such exotic fermions are made massive by introducing brane localized fermions with conjugate  $SU(2) \times U(1)$  charges and an opposite chirality to the exotic fermions, allowing us to write mass terms on the orbifold fixed points. In the GHU scenario, the Yukawa interaction is unified with the gauge interaction, so that the SM fermions obtain the mass of the order of the

<sup>1</sup>It is known that the correct Weinberg angle can also be obtained by introducing brane localized gauge kinetic terms [12], but we do not take this approach in this paper.

$W$ -boson mass after the electroweak symmetry breaking. To realize light SM fermion masses, one may introduce  $Z_2$ -parity odd bulk mass terms for the SM fermions, except for the top quark. Then, zero-mode fermion wave functions with opposite chirality are localized towards the opposite orbifold fixed points and as a result, their Yukawa coupling is exponentially suppressed by the overlap integral of the wave functions. In this way, all exotic fermion zero modes become heavy and small Yukawa couplings for light SM fermions are realized by adjusting the bulk mass parameters. In order to realize the top quark Yukawa coupling, we introduce a rank 4 tensor representation, namely, a symmetric  $\bar{\mathbf{15}}$  without a bulk mass [13]. This leads to a group theoretical factor 2 enhancement of the top quark mass as  $m_t = 2m_W$  at the compactification scale [12]. Note that this mass relation is desirable since the top quark pole mass receives QCD threshold corrections which push up the mass about 10 GeV. See, for example, Ref. [15] for flavor mixing and  $CP$  violation in the GHU scenario.

### A. Higgs boson production through gluon fusion

At the LHC the Higgs boson is dominantly produced via a gluon fusion process with the following dimension 5 operator between the Higgs and digluon:

$$\mathcal{L}_{\text{eff}} = h C_{gg} G_{\mu\nu}^a G^{a\mu\nu} \quad (3)$$

where  $h$  is the SM Higgs boson, and  $G_{\mu\nu}^a$  ( $a = 1-8$ ) is the gluon field strength. With the setup discussed above, we calculate the coefficient of this operator  $C_{gg}$  in our model. The SM contribution to  $C_{gg}$  is dominated by top quark 1-loop corrections. As a good approximation, we express the contribution by using the Higgs low energy theorem [16],

$$C_{gg}^{\text{SMtop}} \simeq \frac{g_3^2}{32\pi^2 v} b_3^t \frac{\partial}{\partial \log v} \log m_t = \frac{\alpha_s}{12\pi v} \quad (4)$$

where  $g_3$  [ $\alpha_s = g_3^2/(4\pi)$ ] is the QCD coupling constant (fine structure constant),  $m_t$  is a top quark mass, and  $b_3^t = 2/3$  is a top quark contribution to the beta function coefficient of QCD.

In addition to the top quark contribution, KK top loop contributions must be taken into account in our model. As mentioned before, the top quark is embedded into the  $\bar{\mathbf{15}}$ -plet with a periodic boundary condition and its KK mass spectrum is given by [13]

$$m_{n,t}^{(\pm)} = m_n \pm 2m_W \quad (5)$$

where  $m_W = 80.4$  GeV is the  $W$ -boson mass,  $m_n \equiv nm_{\text{KK}}$  with an integer  $n = 1, 2, 3, \dots$  and the compactification scale/the unit of KK mode mass  $m_{\text{KK}} = 1/R$ . Although the  $\bar{\mathbf{15}}$ -plet includes exotic massless fermions, we assume that all the exotic fermions are decoupled by adjusting large brane-localized mass terms with the brane fermions

as discussed above. Thus, we only consider KK modes of the SM top quark.<sup>2</sup> It is straightforward to calculate KK top contributions by using the Higgs low energy theorem:

$$\begin{aligned}
C_{gg}^{\text{KKtop}} &\simeq \frac{\alpha_s}{12\pi v} \sum_{n=1}^{\infty} \frac{\partial}{\partial \log v} [\log(m_n + 2m_W) \\
&\quad + \log(m_n - 2m_W)] \\
&= \frac{\alpha_s}{12\pi v} \sum_{n=1}^{\infty} \left[ \frac{2m_W}{m_n + 2m_W} - \frac{2m_W}{m_n - 2m_W} \right] \\
&\simeq -\frac{\alpha_s}{12\pi v} 2 \sum_{n=1}^{\infty} \left( \frac{2m_W}{m_n} \right)^2 \\
&= -\frac{\alpha_s}{12\pi v} \times \frac{\pi^2}{3} \left( \frac{2m_W}{m_{\text{KK}}} \right)^2, \tag{6}
\end{aligned}$$

where we have used an approximation  $m_W^2 \ll m_n^2$  and  $\sum_{n=1}^{\infty} 1/n^2 = \pi^2/6$ . Note that the KK top contribution in the gluon fusion amplitude is destructive to the SM one and finite [8]. This is because of the sign difference between  $m_{n,t}^{(+)}$  and  $m_{n,t}^{(-)}$ , which plays a crucial role to make the KK loop corrections finite.<sup>3</sup> This destructive contribution is a typical feature of the GHU, in sharp contrast with the one in the universal extra dimension models [17]. Now the ratio of the Higgs production cross section in our model to the SM one is estimated as

$$R_\sigma \equiv \left( 1 + \frac{C_{gg}^{\text{KKtop}}}{C_{gg}^{\text{SMtop}}} \right)^2 \simeq \left( 1 - \frac{\pi^2}{3} \left( \frac{2m_W}{m_{\text{KK}}} \right)^2 \right)^2. \tag{7}$$

## B. Higgs decay to diphoton

Next we calculate the KK model contributions to the Higgs-to-diphoton coupling of the dimension 5 operator,

$$\mathcal{L}_{\text{eff}} = h C_{\gamma\gamma} F_{\mu\nu} F^{\mu\nu}, \tag{8}$$

where  $F_{\mu\nu}$  denotes the photon field strength. The coefficient can also be extracted from the 1-loop RGE of the QED gauge coupling by using the Higgs low energy theorem. The diphoton coupling is induced by two contributions via top quark loop and  $W$ -boson loop corrections.

### 1. Top quark loop contributions

As a good approximation, top loop contribution is calculated by

<sup>2</sup>One might think that the KK mode contributions from the light fermions should be taken into account. However, they can be safely neglected compared to those from the heavy fermions since the total KK mode sum is proportional to their fermion masses generated by the electroweak symmetry breaking as is seen in (6) for instance.

<sup>3</sup>This finiteness is shown to be valid in various space-time dimensions and at any perturbative level similar to the Higgs potential in GHU [9].

$$C_{\gamma\gamma}^{\text{SMtop}} \simeq \frac{e^2 b_1'}{24\pi^2 v} \frac{\partial}{\partial \log v} \log m_t = \frac{2\alpha_{\text{em}}}{9\pi v}, \tag{9}$$

where  $b_1 = (2/3)^2 \times 3 = 4/3$  is a top quark contribution to the QED beta function coefficient, and  $\alpha_{\text{em}}$  is the fine structure constant. Corresponding KK top quark contribution is given by

$$\begin{aligned}
C_{\gamma\gamma}^{\text{KKtop}} &\simeq \frac{e^2 b_1'}{24\pi^2 v} \sum_{n=1}^{\infty} \frac{\partial}{\partial \log v} [\log(m_n + m_t) + \log(m_n - m_t)] \\
&\simeq -\frac{2\alpha_{\text{em}}}{9\pi v} \times \frac{\pi^2}{3} \left( \frac{2m_W}{m_{\text{KK}}} \right)^2. \tag{10}
\end{aligned}$$

As in the case of the Higgs-to-digluon coupling, the KK top contribution is destructive to the SM top contribution.

### 2. W-boson loop contributions

The SM  $W$ -boson loop contribution is calculated as

$$C_{\gamma\gamma}^W \simeq \frac{e^2}{32\pi^2 v} b_1^W \frac{\partial}{\partial \log v} \log m_W = -\frac{7\alpha_{\text{em}}}{8\pi v} \tag{11}$$

where  $m_W = g_2 v/2$ , and  $b_1^W = -7$  is a  $W$ -boson contribution to the QED beta function coefficient. This is a rough estimation of the  $W$ -boson loop contributions since  $4m_W^2/m_h^2 \gg 1$  is not well satisfied. For our numerical analysis in the following, we actually use known loop functions for the top quark and  $W$ -boson loop corrections.

In our model, the KK mode mass spectrum of the  $W$ -boson is given by

$$m_{n,W}^{(\pm)} = m_n \pm m_W, \tag{12}$$

so that the contribution from KK  $W$ -boson loop diagrams is found to be

$$\begin{aligned}
C_{\gamma\gamma}^{\text{KKW}} &= \frac{e^2}{32\pi^2 v} b_1^W \sum_{n=1}^{\infty} \frac{\partial}{\partial \log v} [\log(m_n + m_W) \\
&\quad + \log(m_n - m_W)] \\
&\simeq \frac{7\alpha_{\text{em}}}{8\pi v} \frac{\pi^2}{3} \left( \frac{m_W}{m_{\text{KK}}} \right)^2. \tag{13}
\end{aligned}$$

Note again that the KK  $W$ -boson contribution is destructive to the SM  $W$ -boson contribution.

Combining these results, we have

$$C_{\gamma\gamma}^{\text{SMtop}} + C_{\gamma\gamma}^W \simeq -\frac{47\alpha_{\text{em}}}{72\pi v}, \tag{14}$$

$$C_{\gamma\gamma}^{\text{KKtop}} + C_{\gamma\gamma}^{\text{KKW}} \simeq -\frac{\alpha_{\text{em}}}{216\pi v} \pi^2 \left( \frac{m_W}{m_{\text{KK}}} \right)^2. \tag{15}$$

Interestingly, there is an accidental cancellation between KK top and KK  $W$ -boson contributions. We find the partial decay width of  $h \rightarrow \gamma\gamma$  of our model to the SM one as

$$R_{\gamma\gamma} \equiv \left(1 + \frac{C_{\gamma\gamma}^{\text{KKtop}} + C_{\gamma\gamma}^{\text{KKW}}}{C_{\gamma\gamma}^{\text{SMtop}} + C_{\gamma\gamma}^{\text{W}}}\right)^2 \simeq \left(1 + \frac{\pi^2}{141} \left(\frac{m_W}{m_{\text{KK}}}\right)^2\right)^2. \quad (16)$$

Because of the accidental cancellation,  $R_{\gamma\gamma}$  is very close to one for, say,  $m_{\text{KK}} \gtrsim 1$  TeV.

### C. $gg \rightarrow h \rightarrow \gamma\gamma$

Let us now estimate the ratio of the signal strength of the process  $gg \rightarrow h \rightarrow \gamma\gamma$  in our model to the one in the SM. Putting all together, we find

$$R \equiv \frac{\sigma(gg \rightarrow h \rightarrow \gamma\gamma)}{\sigma(gg \rightarrow h \rightarrow \gamma\gamma)_{\text{SM}}} = R_\sigma \times R_{\gamma\gamma} \simeq 1 - \frac{374}{141} \pi^2 \left(\frac{m_W}{m_{\text{KK}}}\right)^2. \quad (17)$$

The result (using loop functions for the SM top and  $W$ -boson loop corrections) is depicted in Fig. 1 as a function of the KK mode mass/the compactification scale. The ratio  $R$  is found to be smaller than 1, because of the destructive KK mode contribution to the gluon fusion channel and the accidental cancellation among the KK mode contributions to the Higgs-to-diphoton decay width. This fact has already been advocated in the previous paper by the present authors [8].

Now we extend the present GHU model to account for the signal strength measured by ATLAS and CMS for the process  $gg \rightarrow h \rightarrow \gamma\gamma$  which is considerably larger than the SM expectation. The simplest extension is to introduce color-singlet bulk fermions with the half-periodic boundary condition,  $\psi(y + 2\pi R) = -\psi(y)$ , in the bulk. The main reasons for this strategy are twofold. The first is that since the KK mode fermion contribution is destructive to the SM fermion contribution, colored KK mode contribution is not desirable for the Higgs production process via gluon fusion. On the other hand, the KK mode contribution

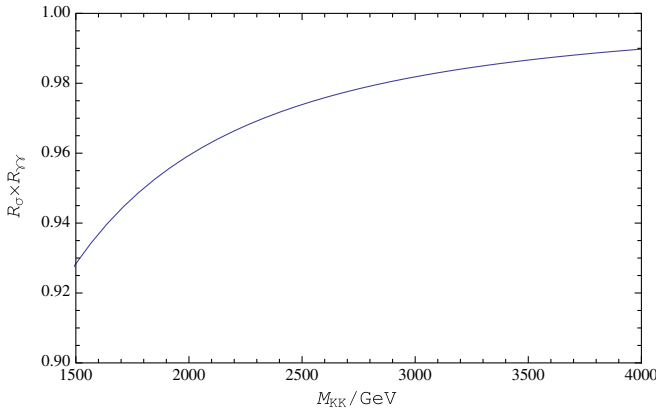


FIG. 1 (color online). The ratio of diphoton events in the simple GHU model to those in the SM as a function of the compactification scale.

is constructive to the SM one for the Higgs-to-diphoton couple. Thus, the introduction of color-singlet bulk fermions nicely work to enhance the diphoton signal strength. The second is that the half-periodic bulk fermion has no massless mode, and unwanted exotic massless fermions do not come out in the model. Another advantage of the half-periodic bulk fermion is that its first KK mode mass is smaller than the compactification scale and its loop corrections dominate over those from the KK modes of the periodic bulk fermion. Furthermore, the existence of the half-periodic bulk fermion is crucial to achieve a Higgs boson mass around 125 GeV in our GHU model, as we will discuss in the next section.

In this paper, we consider two examples for the color-singlet bulk fermions of the representations **10** and **15** of  $SU(3)$ , with a suitable  $U(1)'$  charge assignment. The **10**-plet of  $SU(3)$  is decomposed into representations under  $SU(2) \times U(1)$  as

$$\mathbf{10} = \mathbf{1}_{-1} \oplus \mathbf{2}_{-1/2} \oplus \mathbf{3}_0 \oplus \mathbf{4}_{1/2}, \quad (18)$$

where the numbers in the subscript denote the  $U(1)$  charges. After the electroweak symmetry breaking of the Higgs doublet ( $H: \mathbf{2}_{1/2}$ ), the KK mass spectrum is found as follows:

$$\begin{aligned} (m_{n,-1}^{(\pm)})^2 &= (m_{n+\frac{1}{2}} \pm 3m_W)^2 + M^2, & (m_{n+\frac{1}{2}} \pm m_W)^2 + M^2, \\ (m_{n,0}^{(\pm)})^2 &= (m_{n+\frac{1}{2}} \pm 2m_W)^2 + M^2, & m_{n+\frac{1}{2}}^2 + M^2, \\ (m_{n,+1}^{(\pm)})^2 &= (m_{n+\frac{1}{2}} \pm m_W)^2 + M^2, \\ (m_{n,+2}^{(\pm)})^2 &= m_{n+\frac{1}{2}}^2 + M^2, \end{aligned} \quad (19)$$

where the numbers in the subscript denote the “electric charges”<sup>4</sup> of the corresponding KK mode fermions,  $m_{n+\frac{1}{2}} = (n + \frac{1}{2})m_{\text{KK}}$  with  $n = 0, 1, 2, \dots$ , and  $M$  is a bulk mass.

Employing the Higgs low energy theorem with these mass spectra, we calculate the **10**-plet KK mode contributions to the Higgs-to-diphoton coupling as

$$C_{\gamma\gamma}^{\text{KK-10}} \simeq (Q-1)^2 F(3m_W) + (Q-1)^2 F(m_W) + Q^2 F(2m_W) + (Q+1)^2 F(m_W) \quad (20)$$

where  $Q$  is a  $U(1)'$  charge for the **10**-plet, and the function  $F(m_W)$  is defined as

<sup>4</sup>Here “electric charges” means by electric charges of  $SU(2) \times U(1) \supset SU(3)$ . A true electric charge of each KK mode is given by a sum of the “electric charge” and  $U(1)'$  charge  $Q$ .

$$\begin{aligned}
 F(m_W) &\equiv \frac{\alpha_{\text{em}}}{6\pi\nu} \sum_{n=1}^{\infty} \frac{\partial}{\partial \log \nu} \left[ \log \sqrt{M^2 + (m_{n+\frac{1}{2}} + m_W)^2} + \log \sqrt{M^2 + (m_{n+\frac{1}{2}} - m_W)^2} \right] \\
 &= \frac{\alpha_{\text{em}}}{6\pi\nu} m_W \sum_{n=0}^{\infty} \left( \frac{m_{n+\frac{1}{2}} + m_W}{(m_{n+\frac{1}{2}} + m_W)^2 + M^2} + \frac{m_{n+\frac{1}{2}} - m_W}{(m_{n+\frac{1}{2}} - m_W)^2 + M^2} \right) \\
 &\simeq -\frac{\alpha_{\text{em}}}{3\pi\nu} \left( \frac{m_W}{m_{\text{KK}}} \right)^2 \sum_{n=0}^{\infty} \frac{(n + \frac{1}{2})^2 - c_B^2}{((n + \frac{1}{2})^2 + c_B^2)^2} = -\frac{\alpha_{\text{em}}}{6\pi\nu} \left( \frac{m_W}{m_{\text{KK}}} \right)^2 \frac{\pi^2}{\cosh(\pi c_B)}.
 \end{aligned} \tag{21}$$

Here we have used the approximation  $m_W^2 \ll m_{\text{KK}}^2$ , and  $c_B \equiv M/m_{\text{KK}}$ .

For the **15**-plet case, the decomposition under  $SU(2) \times U(1)$  is given as

$$\mathbf{15} = \mathbf{1}_{-4/3} \oplus \mathbf{2}_{-5/6} \oplus \mathbf{3}_{-1/3} \oplus \mathbf{4}_{1/6} \oplus \mathbf{5}_{2/3}. \tag{22}$$

After the electroweak symmetry breaking, the KK mass spectrum is found as follows:

$$\begin{aligned}
 (m_{n,-4/3}^{(\pm)})^2 &= (m_{n+\frac{1}{2}} \pm 4m_W)^2 + M^2, & (m_{n+\frac{1}{2}} \pm 2m_W)^2 + M^2, & & m_{n+\frac{1}{2}}^2 + M^2, \\
 (m_{n,-1/3}^{(\pm)})^2 &= (m_{n+\frac{1}{2}} \pm 3m_W)^2 + M^2, & (m_{n+\frac{1}{2}} \pm m_W)^2 + M^2, & & (m_{n,2/3}^{(\pm)})^2 = (m_{n+\frac{1}{2}} \pm 2m_W)^2 + M^2, & & m_{n+\frac{1}{2}}^2 + M^2, \\
 (m_{n,5/3}^{(\pm)})^2 &= (m_{n+\frac{1}{2}} \pm m_W)^2 + M^2, & (m_{n,8/3}^{(\pm)})^2 = m_{n+\frac{1}{2}}^2 + M^2, & & & & 
 \end{aligned} \tag{23}$$

where the numbers in the subscript denote the electric charges of the corresponding KK fermions. In this case, the Higgs-to-diphoton coupling is calculated as

$$\begin{aligned}
 C_{\gamma\gamma}^{\text{KK-15}} &\simeq (Q - 4/3)^2 F(4m_W) + (Q - 4/3)^2 F(2m_W) + (Q - 1/3)^2 F(3m_W) \\
 &\quad + (Q - 1/3)^2 F(m_W) + (Q + 2/3)^2 F(2m_W) + (Q + 5/3)^2 F(m_W).
 \end{aligned} \tag{24}$$

For the two cases, we plot the ratio  $R$  as a function of the KK mode mass  $m_{\text{KK}}$  in Fig. 2. The left panel corresponds to the case with the **10**-plet bulk fermion, where we have fixed  $Q = -1$  and  $c_B = 0.23$ . As we will see in the next section, the Higgs boson mass around 125 GeV can be reproduced with the bulk mass  $c_B = 0.23$  for  $m_{\text{KK}} = 3$  TeV. The result for the case with the **15**-plet bulk fermion is depicted in the right panel for  $Q = -5$  and  $c_B = 0.69$ . This bulk mass reproduces the Higgs boson mass around 125 GeV. We find the Higgs-to-diphoton signal strength is considerably

enhanced in the presence of the half-periodic bulk fermions with the TeV scale mass.

As can be understood from Eqs. (20) and (24), the rate of the enhancement depends on the choice of  $U(1)'$  charge  $Q$ . In other words, it can be large as we like by adjusting a  $U(1)'$  charge. In Fig. 3, we plot the ratio of diphoton signal strength to the SM one as a function of the  $U(1)'$  charge  $Q$ , for the two cases. For each plot, the bulk masses are fixed to be the same values as in the previous plots. We can see that  $|Q| = \mathcal{O}(1)$  is enough to give rise to an order 10%

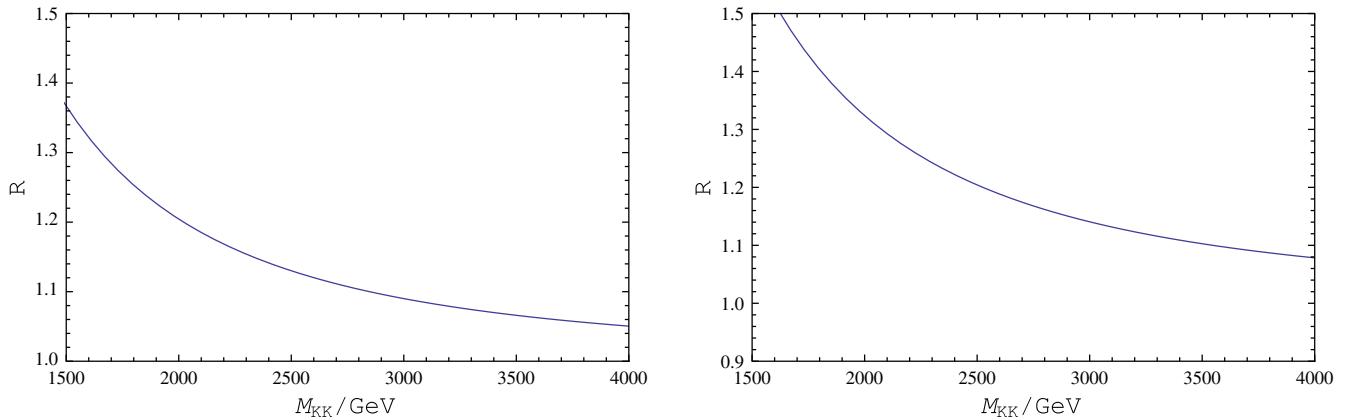


FIG. 2 (color online). The diphoton signal strength (normalized by the SM prediction) in the GHU model with the **10**-plet (left) and **15**-plet (right) bulk fermions as a function of the compactification scale. Here we have used  $Q = -1$  and  $c_B = 0.23$  for the left panel, while  $Q = -5$  and  $c_B = 0.69$  for the right panel.

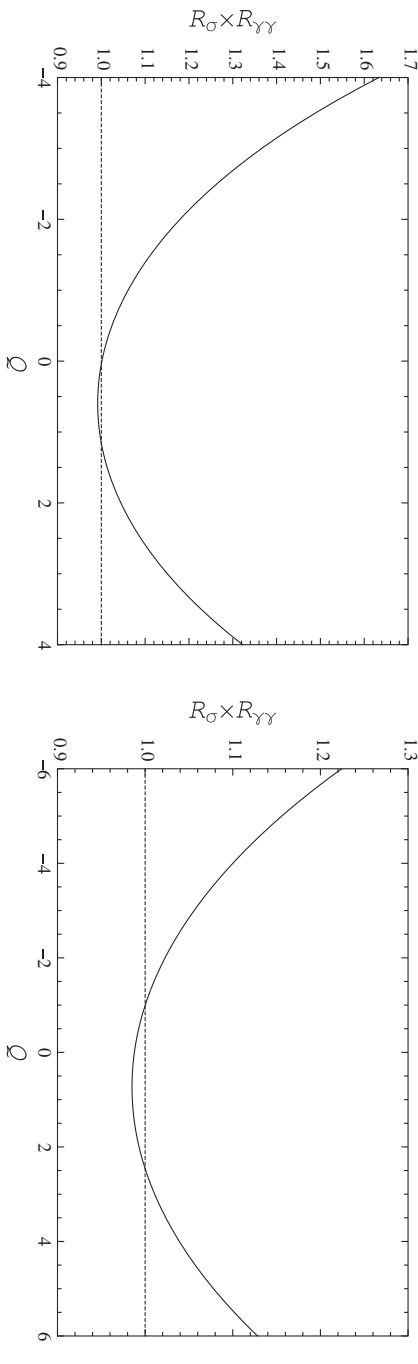


FIG. 3. The diphoton signal strength (normalized by the SM prediction) in the GHU model with the **10**-plet (left) and **15**-plet (right) bulk fermions as a function of the  $U(1)'$  charge  $Q$ , for  $m_{\text{KK}} = 3$  TeV. The bulk masses are fixed as  $c_B = 0.23$  for the left panel, while  $c_B = 0.69$  for the right panel.

enhancement of the diphoton signal. In general, a larger representation field leads to more enhancements than those by smaller representations, since large representations include more fields with higher  $U(1)$  charges in the SM decomposition. In Fig. 3, the deviation of the diphoton signal strength for the case with the **15**-plet fermion is milder than the case with the **10**-plet. This is because a large bulk mass is assigned for the case with the **15**-plet fermion and the KK modes are heavier.

### III. ESTIMATE OF HIGGS BOSON MASS

In this section, we discuss how the Higgs boson mass around 125 GeV is realized in our model. Realizing the 125 GeV Higgs boson mass as well as the electroweak symmetry breaking is quite a nontrivial phenomenological issue in the 5-dimensional GHU scenario. This is because the Higgs doublet is embedded in the 5-dimensional component of the bulk gauge field and as a result, the Higgs doublet has no scalar potential at the tree level. The electroweak symmetry should be broken dynamically, in other words, at the quantum level. In addition, a calculated Higgs boson mass is most likely to be small, since the Higgs quartic coupling is generated at loop levels. Towards a realistic GHU scenario, a variety of extra bulk fields with suitable boundary conditions and bulk/brane mass terms have been considered (see, for example, Refs. [12,13]). It is a highly nontrivial task to propose a simple and phenomenologically viable GHU model.

In estimating the Higgs boson mass, we take a 4-dimensional effective theory approach developed by Ref. [14]. As has been shown in this paper, the low energy effective theory of the 5-dimensional GHU scenario is equivalent to the SM with the so-called gauge-Higgs condition on the Higgs quartic coupling; namely, we impose a vanishing Higgs quartic coupling at the compactification scale. This boundary condition reflects the 5-dimensional gauge invariance which gets restored at an energy higher

than the compactification scale. Employing this effective theory approach, the Higgs boson mass at low energies is easily calculated by solving the RGE of the Higgs quartic coupling with the gauge-Higgs condition, instead of calculating the Coleman-Weinberg potential of the Higgs doublet. We assume that the electroweak symmetry breaking correctly occurs by the introduction of a suitable set of bulk fermions. Note that the effective Higgs mass squared is quadratically sensitive to the mass of heavy states, while the effective Higgs quartic coupling is dominantly determined by interactions of the Higgs doublet with light states. Therefore, the Higgs boson mass at low energies is mainly determined by light states below the compactification scale, once we assume the correct electroweak symmetry breaking. In our model, we have introduced bulk fermions with the half-periodic boundary condition, and their first KK modes appear below the compactification scale. Therefore, not only the SM particles but also the first KK modes are involved in our RGE analysis with the gauge-Higgs condition.<sup>5</sup> The 1-loop RGE for the Higgs quartic coupling  $\lambda$  below the compactification scale is given by

$$\begin{aligned} \frac{d\lambda}{d \ln \mu} = & \frac{1}{16\pi^2} \left[ 12\lambda^2 - \left( \frac{9}{5}g_1^2 + 9g_2^2 \right) \lambda \right. \\ & + \frac{9}{4} \left( \frac{3}{25}g_4^4 + \frac{2}{5}g_1^2g_2^2 + g_2^4 \right) \\ & + 4 \left( 3y_t^2 + C_2(\mathbf{R}) \left( \frac{g_2}{\sqrt{2}} \right)^2 \right) \lambda \\ & \left. - 4 \left( 3y_t^4 + C_4(\mathbf{R}) \left( \frac{g_2}{\sqrt{2}} \right)^4 \right) \right], \end{aligned} \quad (25)$$

where  $y_t$  is the top Yukawa coupling;  $g_{1,2}$  are the  $SU(2)$ ,  $U(1)'$  gauge couplings, respectively; and  $C_2(\mathbf{R})$  and

<sup>5</sup>In Ref. [18], the gauge-Higgs condition with only the SM particle contents below the compactification scale is used to predict the Higgs boson mass.

$C_4(\mathbf{R})$  are contributions to the beta function by the representation  $\mathbf{R} = \mathbf{10}$  or  $\mathbf{15}$ . In our RGE analysis, we neglect the KK mode mass splitting by the electroweak symmetry breaking and set the first KK mode mass as

$$m_0^{(\pm)} = \frac{1}{2} m_{\text{KK}} \sqrt{1 + 4c_B^2}. \quad (26)$$

For the energy scale  $m_0^{(\pm)} \leq \mu \leq m_{\text{KK}}$ , the coefficients  $C_2(\mathbf{R})$  and  $C_4(\mathbf{R})$  are explicitly given by

$$\begin{aligned} C_2(\mathbf{10}) &= 2(3^2 + 1^2 + 2^2 + 1^2), \\ C_4(\mathbf{10}) &= 2(3^4 + 1^4 + 2^4 + 1^4), \\ C_2(\mathbf{15}) &= 2(4^2 + 2^2 + 3^2 + 1^2 + 2^2 + 1^2), \\ C_4(\mathbf{15}) &= 2(4^4 + 2^4 + 3^4 + 1^4 + 2^4 + 1^4), \end{aligned} \quad (27)$$

while these coefficients are set to be 0 for  $\mu < m_0^{(\pm)}$ . In our analysis, the running effects for  $y_t$ ,  $g_{1,2}$  are simply neglected.

The numerical results of 1-loop RGE of the Higgs quartic coupling are shown in Fig. 4. Here we have applied the gauge-Higgs condition at the compactification scale  $1/R = m_{\text{KK}} = 3$  TeV and numerically solved the RGE toward low energies. In the analysis, we have used  $y_t(\mu) = 0.943$  for  $\mu \geq m_t = 173.1$  GeV [ $y_t(\mu) = 0$  for  $\mu < m_t = 173.1$  GeV], and  $g_1 = 0.459$ , and  $g_2 = 0.649$  at the  $Z$ -boson mass scale. For simplicity, we estimate the Higgs boson pole mass by the condition  $\lambda(\mu = m_h)v^2 = m_h^2$ . In Fig. 4, the bulk masses of the  $\mathbf{10}$ -plet and the  $\mathbf{15}$ -plet are fixed to be the values used in the previous section,  $c_B = 0.23$  and  $c_B = 0.69$ , respectively, with which a Higgs boson mass of  $m_h = 125$  GeV [equivalently,  $\lambda(\mu = m_h) = 0.258$ ] is realized. The solid (dashed) line represents the running Higgs quartic coupling for the case with the  $\mathbf{10}$ -plet ( $\mathbf{15}$ -plet) bulk fermion, while the dotted line corresponds to the RGE running in the SM case with the boundary condition  $\lambda(\mu = m_h) = 0.258$ . In this rough analysis, the Higgs quartic coupling becomes zero at  $\mu \sim 10^{4.5}$  GeV. As is well known, in more precise analysis with higher order corrections (see, for example, [19]), the Higgs quartic coupling becomes zero at  $\mu \sim 10^{10}$  GeV. In the precise analysis, the running top Yukawa coupling is monotonically decreasing and the higher order corrections positively contribute to the beta function; as a result, the scale realizing  $\lambda(\mu) = 0$  is pushed up to high energies.

As can be seen from Fig. 4, the existence of the half-periodic bulk fermions is essential to realize the Higgs mass around 125 GeV with the compactification at the TeV scale. Since the bulk fermions provide many first KK mode fermions in the SM decomposition, the running Higgs quartic coupling is sharply rising from zero toward low energies. In addition, the bulk mass also plays a crucial role to adjust the resultant Higgs boson mass to be 125 GeV.

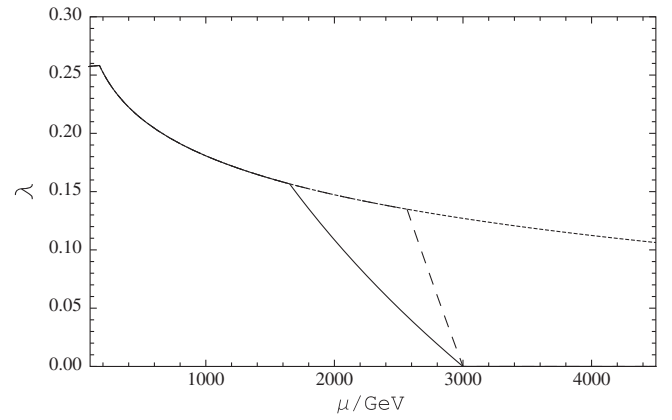


FIG. 4. 1-loop RGE running of the Higgs quartic coupling. The solid (dashed) line corresponds to the case of the  $\mathbf{10}$ -plet ( $\mathbf{15}$ -plet) bulk fermion with the bulk mass  $c_B = 0.23$  ( $c_B = 0.69$ ). Here the compactification scale is fixed as  $m_{\text{KK}} = 1/R = 3$  TeV, at which the gauge-Higgs condition [ $\lambda(m_{\text{KK}}) = 0$ ] is applied. The dotted line shows the running of the SM Higgs quartic coupling with the boundary condition,  $\lambda(\mu = m_h) = 0.258$ , corresponding to the Higgs pole mass  $m_h = 125$  GeV.

#### IV. CONCLUSION

In this paper, we have revisited the Higgs boson production via gluon fusion and its diphoton decay process in a 5-dimensional  $SU(3) \times U(1)'$  GHU model. As shown in [8] and reconfirmed in this paper, the diphoton signal events are reduced in a simple GHU model with only the KK modes of the SM top quark and  $W$ -boson taken into account. As a simple extension of the simple model, we have introduced color-singlet bulk fermions with the half-periodic boundary condition and bulk masses. For concreteness, we have considered the  $SU(3)$   $\mathbf{10}$ -plet and the  $\mathbf{15}$ -plet with a  $U(1)'$  charge  $Q$ . With the charge  $Q$  being of order 1, the diphoton signal events can be remarkably enhanced from the SM prediction by 1-loop corrections of the KK modes at the TeV scale. The signal significance of the diphoton events observed at ATLAS and CMS shows a positive deviation from the SM expectation and it can be an indirect signal of the GHU model. The bulk fermions also play a crucial role to yield the observed Higgs boson mass around 125 GeV. Employing the gauge-Higgs condition, we have shown in the RGE analysis that a Higgs boson mass, which is predicted to be too small in the simple GHU model, is dramatically enhanced in the presence of the half-periodic bulk fermions and the 125 GeV Higgs boson mass is reproduced by adjusting the fermion bulk masses.

There was an interesting argument of naturalness in Ref. [20] that if a large diphoton signal excess is caused by extra fermions having strong couplings with the Higgs boson, the Higgs potential becomes unstable far beneath the 10 TeV scale. In order to keep the Higgs potential stable up to a very high energy, we need a new light scalar field with a strong coupling to the Higgs doublet, which positively contributes to the beta function of the Higgs quartic

coupling. One may think that the existence of such a new light scalar field makes the Standard Model more unnatural [20]. However, note that in the 5-dimensional GHU model, the vanishing of the running Higgs quartic coupling does not indicate the instability of the Higgs potential but instead, the restoration of the bulk gauge symmetry which should occur at an energy higher than the compactification scale. Therefore, the GHU scenario offers a natural solution to the instability of the Higgs potential.

There is another interesting feature of our model. As discussed in [21] (see also [22]), the lightest KK mode of the half-periodic bulk fermion, independently of the background metric, is stable in the effective 4-dimensional theory due to the remaining accidental discrete symmetry. Thus, if its electric charge is arranged to be 0, the lightest KK mode becomes a good candidate for the dark matter in the present Universe. For detailed discussion on the dark

matter physics in the GHU model, we refer the reader to Ref. [21].

One may be also interested in the KK mode contributions to the  $h \rightarrow Z\gamma$  process and its correlation to the  $h \rightarrow \gamma\gamma$  process. However, it seems that the analysis is not so straightforward since the Higgs low energy theorem for  $h \rightarrow Z\gamma$  is not very clear and the corresponding loop functions are complicated. We leave this subject for future study.

## ACKNOWLEDGMENTS

The work of N.M. is supported in part by the Grant-in-Aid for Scientific Research from the Ministry of Education, Science and Culture, Japan No. 24540283 and by Keio Gijuku Academic Development Funds. The work of N.O. is supported in part by the DOE Grant No. DE-FG02-10ER41714.

- 
- [1] G. Aad *et al.* (ATLAS Collaboration), *Phys. Lett. B* **716**, 1 (2012).
- [2] S. Chatrchyan *et al.* (CMS Collaboration), *Phys. Lett. B* **716**, 30 (2012).
- [3] M. Carena, S. Gori, N.R. Shah, and C.E.M. Wagner, *J. High Energy Phys.* **03** (2012) 014; [arXiv:1211.6136](#); J.-J. Cao, Z.-X. Heng, J.M. Yang, Y.-M. Zhang, and J.-Y. Zhu, *J. High Energy Phys.* **03** (2012) 086; M. Carena, S. Gori, N.R. Shah, C.E.M. Wagner, and L.-T. Wang, *J. High Energy Phys.* **07** (2012) 175; H. An, T. Liu, and L.-T. Wang, *Phys. Rev. D* **86**, 075030 (2012); N. Haba, K. Kaneta, Y. Mimura, and R. Takahashi, *Phys. Lett. B* **718**, 1441 (2013); M. A. Ajaib, I. Gogoladze, and Q. Shafi, *Phys. Rev. D* **86**, 095028 (2012); K. Schmidt-Hoberg and F. Staub, *J. High Energy Phys.* **10** (2012) 195; R. Sato, K. Tobioka, and N. Yokozaki, *Phys. Lett. B* **716**, 441 (2012); T. Kitahara, *J. High Energy Phys.* **11** (2012) 021; M. Berg, I. Buchberger, D. M. Ghilencea, and C. Petersson, [arXiv:1212.5009](#).
- [4] B. Batell, S. Gori, and L.-T. Wang, *J. High Energy Phys.* **06** (2012) 172; S. Kanemura and K. Yagyu, *Phys. Rev. D* **85**, 115009 (2012); L. Wang and X.-F. Han, *J. High Energy Phys.* **05** (2012) 088; A. G. Akeroyd and S. Moretti, *Phys. Rev. D* **86**, 035015 (2012); W.-F. Chang, J.N. Ng, and J. M. S. Wu, *Phys. Rev. D* **86**, 033003 (2012); M. Carena, I. Low, and C.E.M. Wagner, *J. High Energy Phys.* **08** (2012) 060; A. Alves, E. Ramirez Barreto, A. G. Dias, C. A. de S. Pires, F.S. Queiroz, and P.S. Rodrigues da Silva, *Eur. Phys. J. C* **73**, 2288 (2013); T. Abe, N. Chen, and H.-J. He, *J. High Energy Phys.* **01** (2013) 082; A. Joglekar, P. Schwaller, and C.E.M. Wagner, *J. High Energy Phys.* **12** (2012) 064; N. Arkani-Hamed, K. Blum, R. T. D’Agnolo, and J. Fan, *J. High Energy Phys.* **01** (2013) 149; L. G. Almeida, E. Bertuzzo, P. A. N. Machado, and R. Z. Funchal, *J. High Energy Phys.* **11** (2012) 085; M. Hashimoto and V.A. Miransky, *Phys. Rev. D* **86**, 095018 (2012); M. Reece, *New J. Phys.* **15**, 043003 (2013); H. Davoudiasl, H.-S. Lee, and W. J. Marciano, *Phys. Rev. D* **86**, 095009 (2012); M. B. Voloshin, *Phys. Rev. D* **86**, 093016 (2012); A. Kobakhidze, [arXiv:1208.5180](#); A. Urbano, *Phys. Rev. D* **87**, 053003 (2013); L. Wang and X.-F. Han, *Phys. Rev. D* **87**, 015015 (2013); E. J. Chun, H. M. Lee, and P. Sharma, *J. High Energy Phys.* **11** (2012) 106; H. M. Lee, M. Park, and W.-I. Park, *J. High Energy Phys.* **12** (2012) 037; L. Wang and X.-F. Han, *Phys. Rev. D* **87**, 015015 (2013); B. Batell, S. Gori, and L.-T. Wang, *J. High Energy Phys.* **01** (2013) 139; M. Chala, *J. High Energy Phys.* **01** (2013) 122; B. Batell, S. Jung, and H. M. Lee, *J. High Energy Phys.* **01** (2013) 135; C.-W. Chiang and K. Yagyu, *J. High Energy Phys.* **01** (2013) 026; H. Davoudiasl, I. Lewis, and E. Ponton, *Phys. Rev. D* **87**, 093001 (2013); M. Aoki, S. Kanemura, M. Kikuchi, and K. Yagyu, *Phys. Rev. D* **87**, 015012 (2013); F. Arbabifard, S. Bahrami, and M. Frank, *Phys. Rev. D* **87**, 015020 (2013); S. Funatsu, H. Hatanaka, Y. Hosotani, Y. Orikasa, and T. Shimotani, *Phys. Lett. B* **722**, 94 (2013); P. S. B. Dev, D. K. Ghosh, N. Okada, and I. Saha, *J. High Energy Phys.* **03** (2013) 150; **05** (2013) 049(E); A. Carmona and F. Goertz, [arXiv:1301.5856](#).
- [5] N. S. Manton, *Nucl. Phys.* **B158**, 141 (1979); D. B. Fairlie, *Phys. Lett.* **82B**, 97 (1979); *J. Phys. G* **5**, L55 (1979); Y. Hosotani, *Phys. Lett.* **126B**, 309 (1983); **129B**, 193 (1983); *Ann. Phys. (N.Y.)* **190**, 233 (1989).
- [6] I. Antoniadis, K. Benakli, and M. Quiros, *New J. Phys.* **3**, 20 (2001); G. von Gersdorff, N. Irges, and M. Quiros, *Nucl. Phys.* **B635**, 127 (2002); R. Contino, Y. Nomura, and A. Pomarol, *Nucl. Phys.* **B671**, 148 (2003); C. S. Lim, N. Maru, and K. Hasegawa, *J. Phys. Soc. Jpn.* **77**, 074101 (2008).
- [7] N. Maru and T. Yamashita, *Nucl. Phys.* **B754**, 127 (2006); Y. Hosotani, N. Maru, K. Takenaga, and T. Yamashita, *Prog. Theor. Phys.* **118**, 1053 (2007).
- [8] N. Maru and N. Okada, *Phys. Rev. D* **77**, 055010 (2008).

- [9] N. Maru, *Mod. Phys. Lett. A* **23**, 2737 (2008).
- [10] Y. Adachi, C. S. Lim, and N. Maru, *Phys. Rev. D* **76**, 075009 (2007); **79**, 075018 (2009).
- [11] Y. Adachi, C. S. Lim, and N. Maru, *Phys. Rev. D* **80**, 055025 (2009).
- [12] C. A. Scrucca, M. Serone, and L. Silvestrini, *Nucl. Phys.* **B669**, 128 (2003).
- [13] G. Cacciapaglia, C. Csaki, and S. C. Park, *J. High Energy Phys.* **03** (2006) 099.
- [14] N. Haba, S. Matsumoto, N. Okada, and T. Yamashita, *J. High Energy Phys.* **02** (2006) 073; *Prog. Theor. Phys.* **120**, 77 (2008).
- [15] Y. Adachi, N. Kurahashi, C. S. Lim, and N. Maru, *J. High Energy Phys.* **11** (2010) 150; **01** (2012) 047; Y. Adachi, N. Kurahashi, N. Maru, and K. Tanabe, *Phys. Rev. D* **85**, 096001 (2012); arXiv:1201.2290; C. S. Lim, N. Maru, and K. Nishiwaki, *Phys. Rev. D* **81**, 076006 (2010).
- [16] J. Ellis, M. K. Gaillard, and D. V. Nanopoulos, *Nucl. Phys.* **B106**, 292 (1976).
- [17] F. J. Petriello, *J. High Energy Phys.* **05** (2002) 003; S. K. Rai, *Int. J. Mod. Phys. A* **23**, 823 (2008).
- [18] I. Gogoladze, N. Okada, and Q. Shafi, *Phys. Lett. B* **655**, 257 (2007); **659**, 316 (2008); B. He, N. Okada, and Q. Shafi, *Phys. Lett. B* **716**, 197 (2012).
- [19] For a recent work, see, for example, G. Degrossi, S. Di Vita, J. Elias-Miro, J. R. Espinosa, G. F. Giudice, G. Isidori, and A. Strumia, *J. High Energy Phys.* **08** (2012) 098.
- [20] N. Arkani-Hamed, K. Blum, R. T. D'Agnolo, and J. Fan, *J. High Energy Phys.* **01** (2013) 149.
- [21] N. Haba, S. Matsumoto, N. Okada, and T. Yamashita, *J. High Energy Phys.* **03** (2010) 064.
- [22] M. Regis, M. Serone, and P. Ullio, *J. High Energy Phys.* **03** (2007) 084; G. Panico, E. Ponton, J. Santiago, and M. Serone, *Phys. Rev. D* **77**, 115012 (2008); M. Carena, A. D. Medina, N. R. Shah, and C. E. M. Wagner, *Phys. Rev. D* **79**, 096010 (2009); Y. Hosotani, P. Ko, and M. Tanaka, *Phys. Lett. B* **680**, 179 (2009).